Int. J. Electrochem. Sci., 12 **(2017)** 1075 – 1093, doi: 10.20964/2017.02.34

International Journal of
ELECTROCHEMICAL
SCIENCE
www.electrochemsci.org

Alloy Formation by Electrodeposition of Niobium and Aluminium on Gold from Chloroaluminate Melts

Nataša M. Vukićević[1], *Vesna S. Cvetković*[1,*], *Ljiljana S. Jovanović*[2], *Sanja I. Stevanović*[1], *Jovan N. Jovićević*[1]

[1] Institute of Chemistry, Technology and Metallurgy, University of Belgrade, Njegoševa 12, 11000 Belgrade, Serbia, PAK 125213
[2] Faculty of Scences, University of Novi Sad, Trg D. Obradovića 3, 21000 N. Sad, Serbia.
[*]E-mail: v.cvetkovic@ihtm.bg.ac.rs.

Received: 3 October 2016 / *Accepted:* 8 December 2016 / *Published:* 30 December 2016

Niobium and aluminium have been electrodeposited from inorganic chloroaluminate melts onto gold substrate at 473 K. The melts were prepared from an equimolar mixture of $AlCl_3$+NaCl with niobium added by anodic dissolution. It was found that aluminium and niobium underpotential deposition on gold precedes overpotential deposition of niobium and subsequent aluminium deposition. Niobium was overpotentially deposited individually and co-deposited with aluminium. Applied electrochemical techniques (linear sweep voltammetry, polarization, open circuit and potential step) indicated, then physical analytical methods (scanning electron microscopy, energy dispersive spectrometry, atomic force microscopy and X-ray diffraction) confirmed formation of several niobium-aluminium, niobium-gold and aluminium-gold alloys in niobium and aluminium underpotential as well as in niobium and aluminium overpotential regions.

Keywords: Niobium, Aluminium, Gold, Metal deposition, Alloy formation, Chloroaluminate melt

1. INTRODUCTION

The wide potential difference decomposition limits of many melts allows the electrodeposition of highly electropositive metals or very electronegative elements [1-3]. The electrochemical methods can produce very pure metals and are generally less polluting than chemical processes and at generally lower operating temperatures. Moreover, at higher temperatures, the deposited metal diffuses into the substrate metal and as a result a compact layer of alloys can be formed [1-2,4,5].

More recently, interest has been focused on preparation of refractory metals by electrochemical deposition, particularly niobium [6,7]. Niobium has unique properties such as a high melting point,

hydrogen absorption capacity, superconductivity and biocompatibility. It is used either as a pure metal or in the form of alloys [7-9]. Nb-Al binary alloys such as Nb_3Al are possible candidates for superconducting wires and $NbAl_3$ for high quality aerospace systems [10,11]. Electrochemical behaviour of niobium in chloride, chloride–fluoride, fluoride and oxofluoride melts has been a subject of numerous studies [1,6,12-22]. Work done by Mohamedi et al. [23] describes the reduction mechanism by which niobium–aluminium alloys are formed in LiCl–KCl eutectic melts. There are reports on the electrochemistry of niobium chloride and oxide-chloride complexes from a basic [EMIm]Cl/$AlCl_3$ ionic liquid [24,25] and electrodeposition of Al-Nb alloys from N-butylpyridinium chloride/$AlCl_3$ containing $NbCl_5$ or Nb_3Cl_8. Electrochemical behaviour of niobium in 1-ethyl-3-methylimidazolium chloride/aluminium chloride was also studied [26,27] and authors succeeded in obtaining Nb-Al alloys but not in extracting pure niobium. Recently it was reported that niobium electrodeposition might be possible from basic mixtures of $NbCl_5$, or NbF_5, and organic ionic liquids electrolytes [28-31]. From this literature, it is evident that the deposition of elemental Nb from ionic liquids is not a straightforward process, and it is difficult to obtain relatively thick layers of niobium deposits.

There is now again increased interest in alkali chlorides which are more cost effective, less toxic and less corrosive than fluorides and majority of other ionic liquids in use. Several studies involving niobium electrodeposition have been conducted in chloroaluminate electrolytes made of $NbCl_5$ in $AlCl_3$-RCl (R = Na, K) [14,17,32-34]. General behaviour reported is the reversible step-wise reduction to Nb(III). Formation of lower oxidation states resulted in dimerization and cluster formation. No evidence of deposition of Nb or Nb-Al alloys from $NbCl_5$ containing melts has been disclosed to date. Sato, [17] however, has reported that deposition from mixtures with added Nb_3Cl_8 to 55 m/o $AlCl_3$-NaCl can lead to Nb-Al alloys containing up to 18 a/o Nb. The limiting factor appears to be the low solubility of Nb_3Cl_8 in the electrolyte. On the other hand, when electroactive niobium species are introduced via anodic dissolution of metallic niobium, significantly higher alloy compositions, up to 35 a/o Nb, were reported [17]. Stafford and Haarberg [34] further examined Nb dissolution in 52 m/o $AlCl_3$ + NaCl and the subsequent deposition of Nb-Al alloys. The Nb content of the alloy varies inversely with the applied current density, suggesting that the niobium deposition reaction is diffusion limited whereas aluminium deposition is under kinetic or mixed control. On the niobium electrode, aluminium in LiCl-KCl-$AlCl_3$ melt showed very complex behaviour: underpotential deposition of aluminium followed by formation of a surface alloy of aluminium–niobium [23]. From chronoamperometric measurements, it was concluded that the niobium electroactive species are not reduced to the metallic form on tungsten until the co-deposition of aluminium begins from LiCl-KCl-$AlCl_3$-Nb_3Cl_8 melt [23].

In the recent years there is growing interest towards studying of processes involving electrodeposition of niobium and aluminium from chloride melts and formation of their alloys. Particular attention is directed to the development of prospective methods of preparation of Nb_3Al and $NbAl_3$ intermetallics. This work is intended to further expand on the work done to date on the topics.

2. EXPERIMENTAL METHODS

2.1. Electrochemical experiments

All electrochemical experiments were performed in a 50 cm^3 three neck borosilicate glass cell with three electrodes, a thermocouple and argon inlet and outlet. Working gold electrodes were rectangular plates (0.5 cm^2 surface area and 0.25 mm thick) and wires (1 mm thick, 99.999% Au, Johnson, Matthey & Co. Ltd. Chemical division). Counter electrode was niobium plate (5 cm^2, 0.5 mm thick, 99.95% Nb, HLMET Co, Ltd.) and reference electrode was aluminium cylindrical rod (3 mm in diameter, 99.999% Al, LTS Chemical Inc.). Electrochemical experiments were performed at 473 K under argon atmosphere, with the cell in a hermetically sealed acrylic glove box, using an EG&G PAR Potentiostat/Galvanostat Model 273A controlled by Power Suite software (Princeton Applied Research).

The electrolyte used was a melt consisting of equimolar mixture of $AlCl_3$+NaCl + anodically dissolved Nb. Only fresh anhydrous $AlCl_3$ (p.a. Merck) was used for each melt preparation. It was placed at the bottom of the cell and covered with NaCl (p.a. Merck), previously dried for 10 hours at 823 K. Mixture was then heated slowly to 473 K until colourless liquid electrolyte was apparent. The liquid electrolyte was then subjected to pre-electrolysis (working electrode 99.999% Pt, Aldrich; counter and reference electrodes 99.999% Al, LTS Chemical Inc.) for 10 hours under current density 0.75 $mAcm^{-2}$ and argon atmosphere. Finally, all the cell electrodes were switched to niobium. Working electrode was dissolved, under argon atmosphere (the current density applied was 150 $mAcm^{-2}$) long enough to secure the wanted Nb concentration [16,34]. Between 1000 and 3000 C was passed through the working Nb anode. Typically dissolved Nb corresponded to an equivalent of about 0.4 to 1.2 mol% of $NbCl_5$ in the melt. This was calculated using the difference in weight loss of the niobium anode dissolved and the charge used in the anode dissolution.

The study started with recording of reversed polarization curves for the gold working electrode whose potential (measured versus aluminium reference electrode) was scanned from the starting value, E_s (50 mV negative to the reversible gold potential) to final value, E_f (0.000 mV or up to several hundred mV negative to the reversible potential of aluminium) and back to E_s at the rate of 1 mVs^{-1}. Cyclic voltammetry experiments were performed at different scan rates within the same potential windows. Some of the cyclic voltammograms were obtained after the final potential (cathodic overpotential end of the potential window, E_f) was held constant for some time before the reverse part of the cycle was performed.

Potentiostatic experiments were carried out within the same potential windows at different final cathodic potential values with the potentials held for 1-6 hours.

After the potential pulses (30-60 minutes), more negative than the reversible potential of niobium or/and aluminium, some working electrodes were switched off the potentiostatic control and left under a constant dissolution current ($2x10^{-5}$ A) to return to their initial reversible potentials. Results of these quasi “open circuit” measurements were changes in the potential of working electrodes, covered with electrodeposited metals or alloys, with respect to time.

2.2. Surface/ sub-surface analysis

Controled electrodeposition onto gold electrode started 5 min after insertion of the working electrode into the melt in order to allow thermal equilibrium. Niobium and aluminium were electrodeposited from chloroaluminate melt enriched with niobium at constant potential (UPD or OPD vs. Al) for different time periods (1, 2, 4, 5 and 4h) at 473 K. After electrodeposition experiments, samples were washed with distilled water and ethanol to remove the residual melt. The structure and quality of the deposits obtained were analyzed using scanning electron microscopy (SEM, JEOL-model JSM-5800), energy dispersive spectroscopy (EDS, Oxford INCA 3.2), X-ray diffraction (XRD, Enraf Nonius powder diffractometer) and atomic force microscopy (AFM with NanoScope 3D Veeco, microscope operated in contact mode under ambient conditions. Silicon Nitride probes with spring constant of 20-80 N/m were used).

3. RESULTS AND DISCUSSION

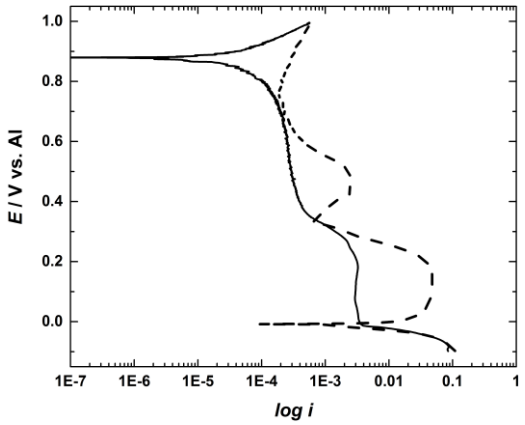

Figure 1. Polarization curves obtained on gold electrode from equimolar $AlCl_3$+NaCl melt containing anodically dissolved Nb; T = 473 K; ν = 1 mV/s; (dotted line) E_s = − 0.100 V vs. Al → E_f = 1.000 V vs. Al; (solid line) E_s = 1.000 V vs. Al → E_f = − 0.100 V vs. Al.

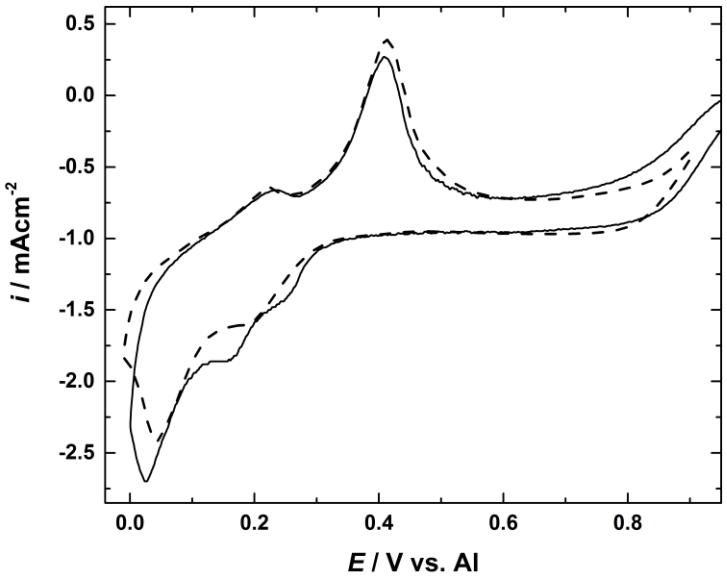

a)

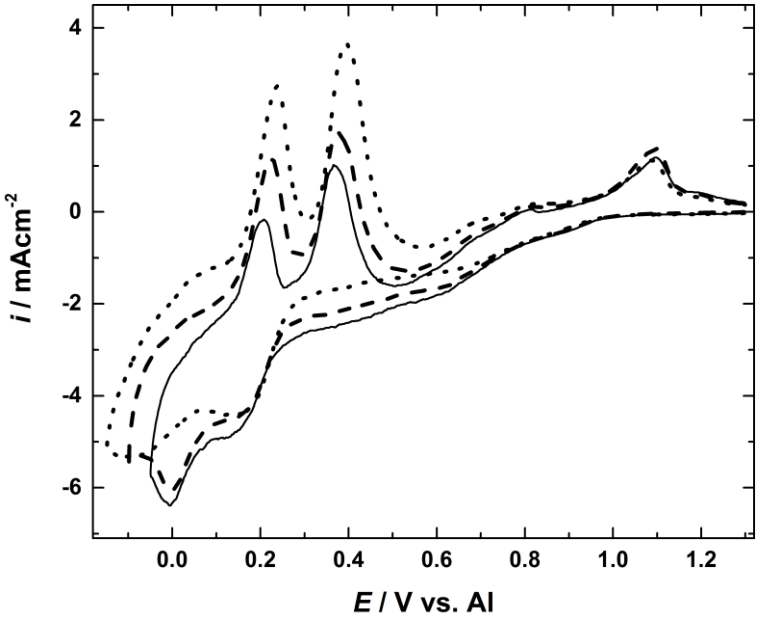

b)

Figure 2. Voltammograms obtained on gold electrode from equimolar $AlCl_3$+NaCl melts with anodically dissolved Nb obtained at 473 K with cathodic end potential in aluminium UPD and entering aluminium OPD region: a) v = 10 mV/s, E_f = 0.000 V vs. Al (solid line); E_f = − 0.020 V vs. Al (dashed line) and b) v = 20 mV/s, E_f = − 0.050 V vs. Al (solid line); E_f = − 0.100 V vs. Al (dashed line); E_f = − 0.150 V vs. Al (dotted line).

Polarization curves recorded on the gold electrode in the potential region between reversible potentials of gold and aluminium, Fig. 1, revealed a number of reversible potentials, but reversible potentials close to or equal to ≈ 0.000 V vs. Al, ≈ 0.280 V vs. Al and ≈ 0.450 V vs. Al. were universally observed.

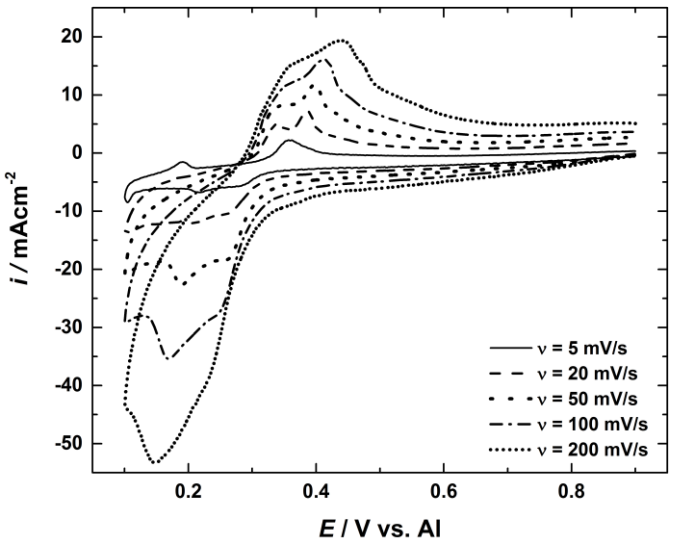

a)

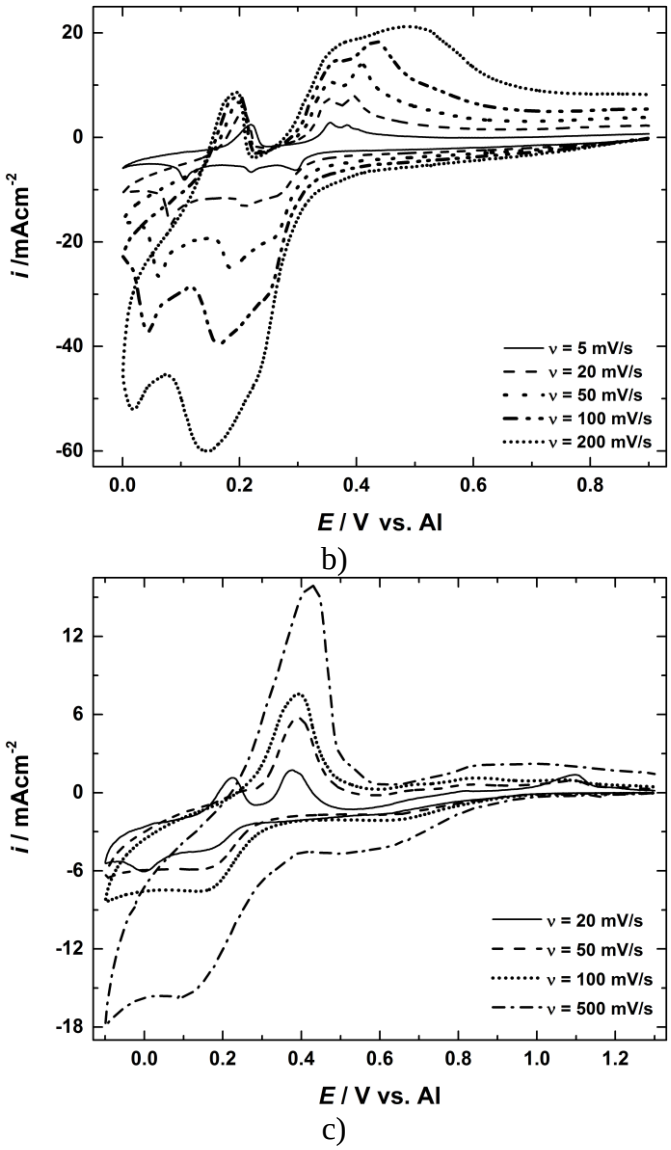

Figure 3. Linear sweep voltammograms obtained with different sweep rates on gold electrode from equimolar $AlCl_3$+NaCl melts with anodically dissolved Nb at 473 K: a) and b) in aluminium UPD region; c) entering aluminium OPD region.

Typical linear sweep voltammograms obtained on the gold working electrode in the aluminium underpotential (UPD) region with final cathodic potential, E_f, entering aluminium overpotential (OPD) region, are presented in Fig. 2.a) and b), respectively. It is worthwhile noting that peak potentials of the cathodic peaks and their anodic counterparts are very close to the values of the above mentioned reversible potentials recorded on the polarization curves (see Fig. 1).

Voltammograms recorded within the same potential range but with different sweep rates are presented in Fig. 3. The $i_{peak} = f(\nu^{1/2})$, $i_{cathodicpeak}/i_{anodicpeak}$ and $E_{cathodicpeak}/E_{anodicpeak}$ analysis for the cathodic peak close to ≈ 0.100 V vs. Al and its anodic counterpart suggests controlled rate of the process at the electrode taking place at those potentials [16,35].

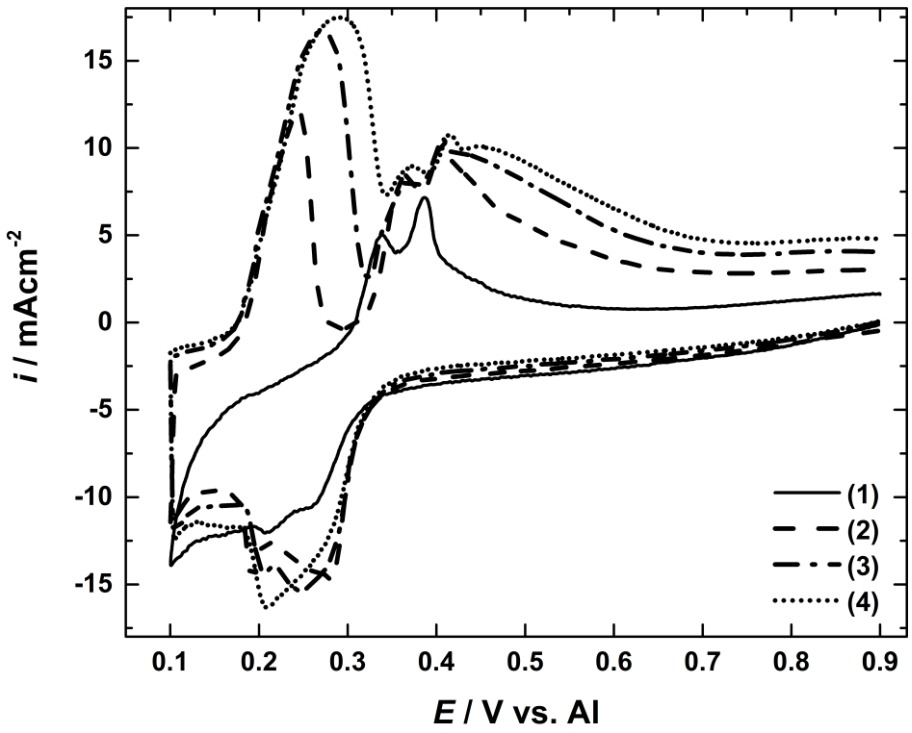

Figure 4. Niobium-aluminium deposition/dissolution on/from gold electrode in equimolar $AlCl_3$+NaCl melts containing anodically dissolved Nb, obtained by niobium deposition at E = 0.100 V vs. Al for 1) 0 s; 2) 60 s; 3) 180 s and 4) 300 s at 473 K (sweep rate 20 mVs^{-1}).

Cyclic voltammograms recorded on the systems with different increasing deposition holds at the cathodic potential, E_f, of 0.100 V vs. Al are displayed in Fig. 4. Prolonged deposition at the potential of 0.100 V vs. Al brings about a slight change in peak potentials (compared to the values obtained by polarization curves and linear sweep voltammetry) and an increase of the currents and charges covered by the anodic counterpart peaks (Table 1.). It should be noted that the two recorded cathodic peaks do not change substantially peak potential values, although they do somewhat change peak currents.

Table 1. Peak potentials *E* (V vs. Al) and corresponding anodic current densities *i* (10^{-3} Acm^{-2}) from the anodic region of linear sweep voltammograms on gold electrodes as a function of deposition time τ_d (s) (Fig. 4).

τ_d (s)	0		60		180		360	
T	*E*	*i*	*E*	*i*	*E*	*i*	*E*	*i*
473 K	-	-	0.247	11.94	0.259	16.26	0.287	17.5
	0.338	5.02	0.354	8.54	0.364	8.1	0.362	8.96
	0.384	7.12	0.400	9.7	0.400	9.7	0.410	10.76

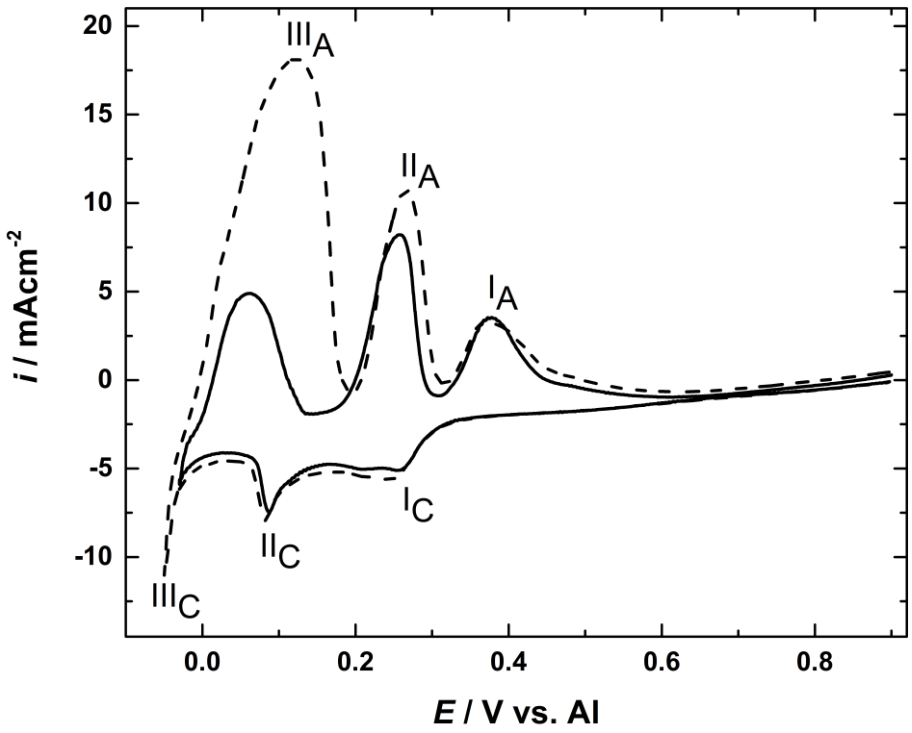

Figure 5. Voltammograms obtained on gold electrode in equimolar $AlCl_3$+NaCl melts with anodically dissolved Nb at 473 K (sweep rate 10 mVs^{-1}) with cathodic potential end held for 60 s at: (solid line) – 0.030 V vs. Al; (dashed line) – 0.050 V vs. Al.

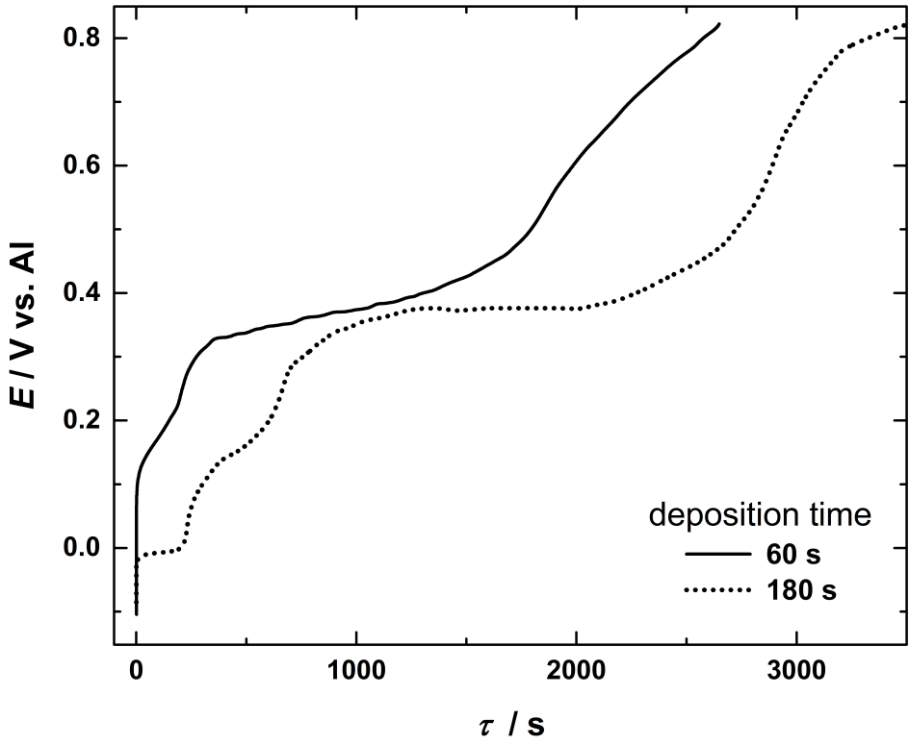

Figure 6. "Open circuit" graphs of niobium-aluminium dissolution from gold electrodes at 473 K, after potentiostatic deposition at E_f = – 0.100 V vs. Al for different times.

When final cathodic potential, E_f, was shifted in the negative direction to 0.000 V vs. Al three distinct cathodic (I_C, II_C, III_C) and three distinct anodic peaks (I_A, II_A, III_A) were recorded (see Fig.5). When the final cathodic potential was pushed further, to larger aluminium cathodic overpotentials (OPD) the current density of the reduction peak at potential close to 0.150 V vs. Al (peak II_C) would not increase but its anodic counterpart (II_A) would. These findings suggest niobium deposition with limited rate and dissolution of the deposited material. Second cathodic peak entering aluminium overpotential range (III_C) reflects aluminium deposition, and anodic peak (III_A) around 0.100 V vs. Al represents dissolution of the deposited aluminium and probably additional niobium. It should be noted that the current of the reduction peak around 0.300 V vs. Al (peak I_C) and its anodic counterpart close to 0.400 V vs. Al (peak I_A) did not increase when either of the above mentioned final cathodic potentials were applied. These peaks should be attributed to aluminium underpotential deposition onto gold [36].

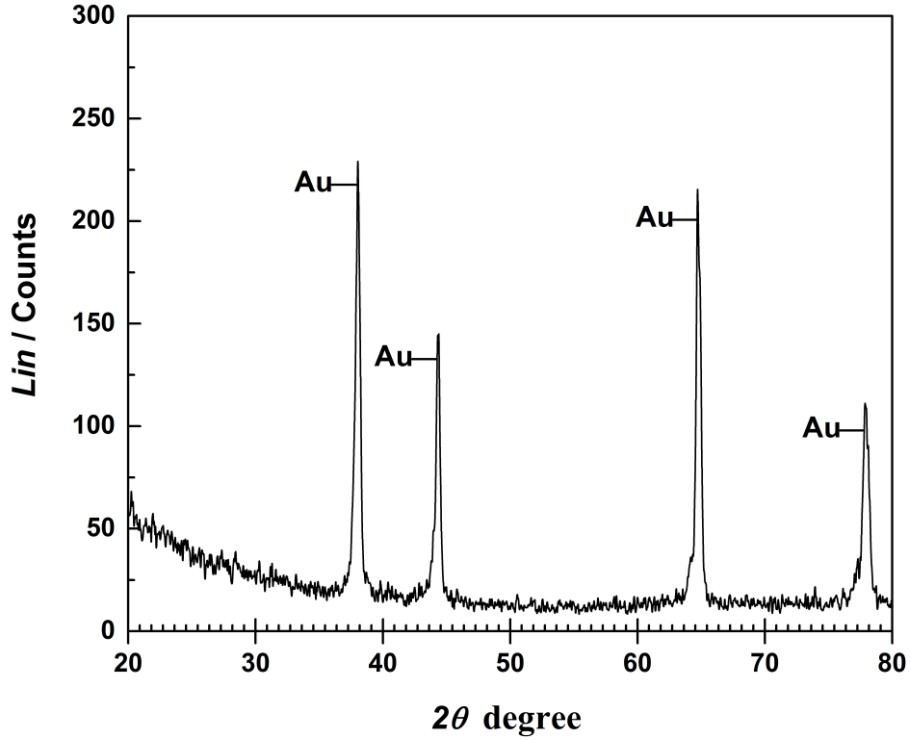

Figure 7. XRD spectra of the gold electrode held for 6 h at E = 0.300V vs. Al in the melt of equimolar mixture $AlCl_3$+NaCl containing anodically dissolved Nb at T = 473 K [39].

Potential-time diagrams of niobium-aluminium dissolution from gold electrodes, obtained by "open circuit measurements" (OC) are given in Figure 6. They reveal plateaux potentials (≈ 0.000 V vs. Al; ≈ 0.150 V vs. Al; ≈ 0.300 V vs. Al) which are very close to the values of the anodic peak potentials obtained by cyclic voltammetry under the same conditions. Each of these plateaux should represent equilibrium potential between a phase on the electrode and its ions in the melt.

The results obtained by the electrochemical techniques used indicate that:

a) at potentials close to 0.250 V vs. Al aluminium underpotential deposition on gold occurs and results in formation of Al-Au alloys [36] which in turn dissolve at potentials close to 0.400 V vs. Al;

b) at potentials close to 0.150 V vs. Al niobium metal deposition commences and soon becomes rate controlled. Niobium dissolves at potentials close to 0.300 V vs. Al;

c) at potentials negative to 0.000 V vs. Al aluminium overpotential deposition occurs and it seems to proceed in addition to the niobium diffusion controlled deposition. The deposited material starts dissolving at potentials close to 0.150 V vs. Al.

Understanding of the results obtained by electrochemical methods was improved by EDS, SEM, AFM and XRD analysis. Fig. 7 presents XRD analysis of the gold electrode exposed to the potential of 0.300 V vs. Al for 6 hours and it should be concluded that there are no well-pronounced peaks other than those belonging to the gold substrate.

An example of XRD spectra for polycrystalline gold electrode exposed to constant potential of 0.150 V vs. Al for 4 hours at 473 K is exhibited in Fig. 8. Apart from the gold peaks there are peaks belonging to Au/Al, Au/Nb and Nb/Al alloys. No niobium peaks were recorded. This suggests that aside from aluminium UPD on gold [36], there could be also niobium UPD on gold [37,38] as well. These underpotential depositions should be responsible for the formation of the alloys recorded. The absence of the niobium bulk metal peaks is understandable on account that used potential is not in the region of cathodic overpotential needed for the metal niobium to be deposited. However, when potential of 0.100 V vs. Al was applied for five hours there was clear evidence of Nb metal being deposited (Fig. 9), apart from a number of Nb/Au alloys and evidence of Al/Nb alloys being formed. It was when the potentials belonging to aluminium cathodic overpotential range were applied, that the evidence of aluminium metal was recorded by XRD as well, Fig. 10a) and b).

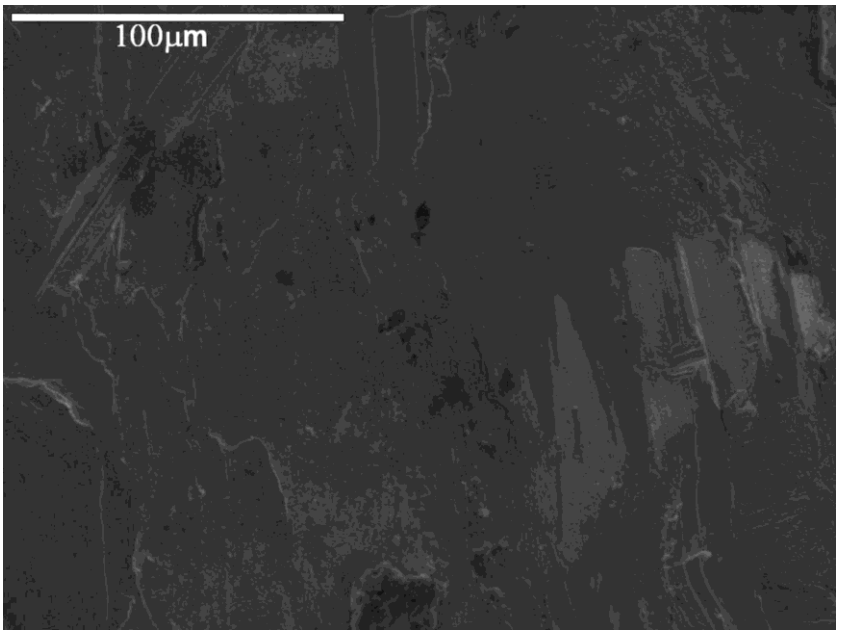

a)

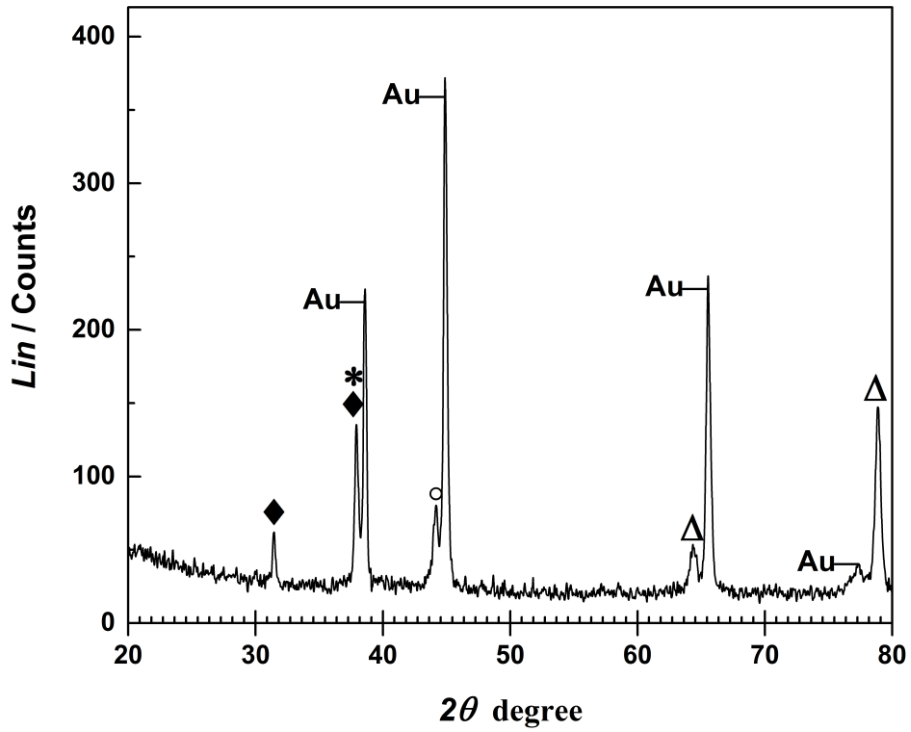

b)

Figure 8. a) SEM photo of the Au surface after 4 h being held at E = 0.150 V vs. Al in the melt of equimolar mixture $AlCl_3$+NaCl with anodically dissolved Nb at T = 473 K (magnification 1000x); b) XRD analysis of the a) sample: **(Au)**-Au [39]; **(♦)**-Au_2Nb_3 [40]; **(*)**-$AlNb_3$ [41]; **(o)**-$AlAu_2$ [42]; **(Δ)**-$AlNb_2$ [43].

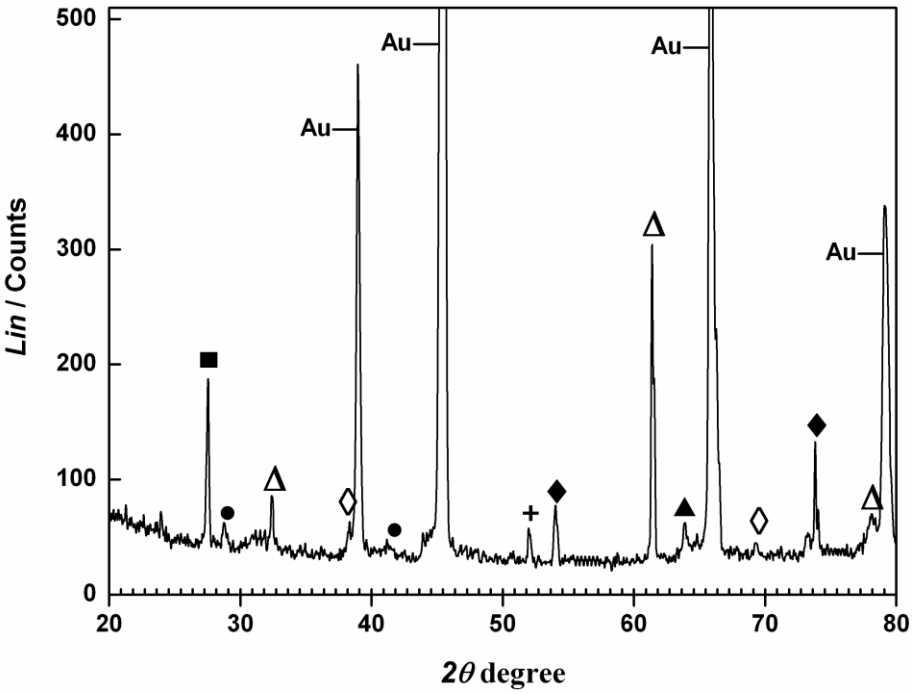

Figure 9. XRD pattern for the Au electrode held for 5 h at E = 0.100V vs. Al in the melt of equimolar mixture $AlCl_3$+NaCl containing anodically dissolved Nb, T = 473 K; **(Au)**-Au [39]; (■)-AlAu [44]; **(●)**-$AlAu_4$ [45]; **(Δ)**-$AlNb_2$ [43]; **(◊)**-Nb [46]; **(+)**-Au_2Nb [47]; **(♦)**-Au_2Nb_3 [40]; **(▲)**-NbO_2 [48].

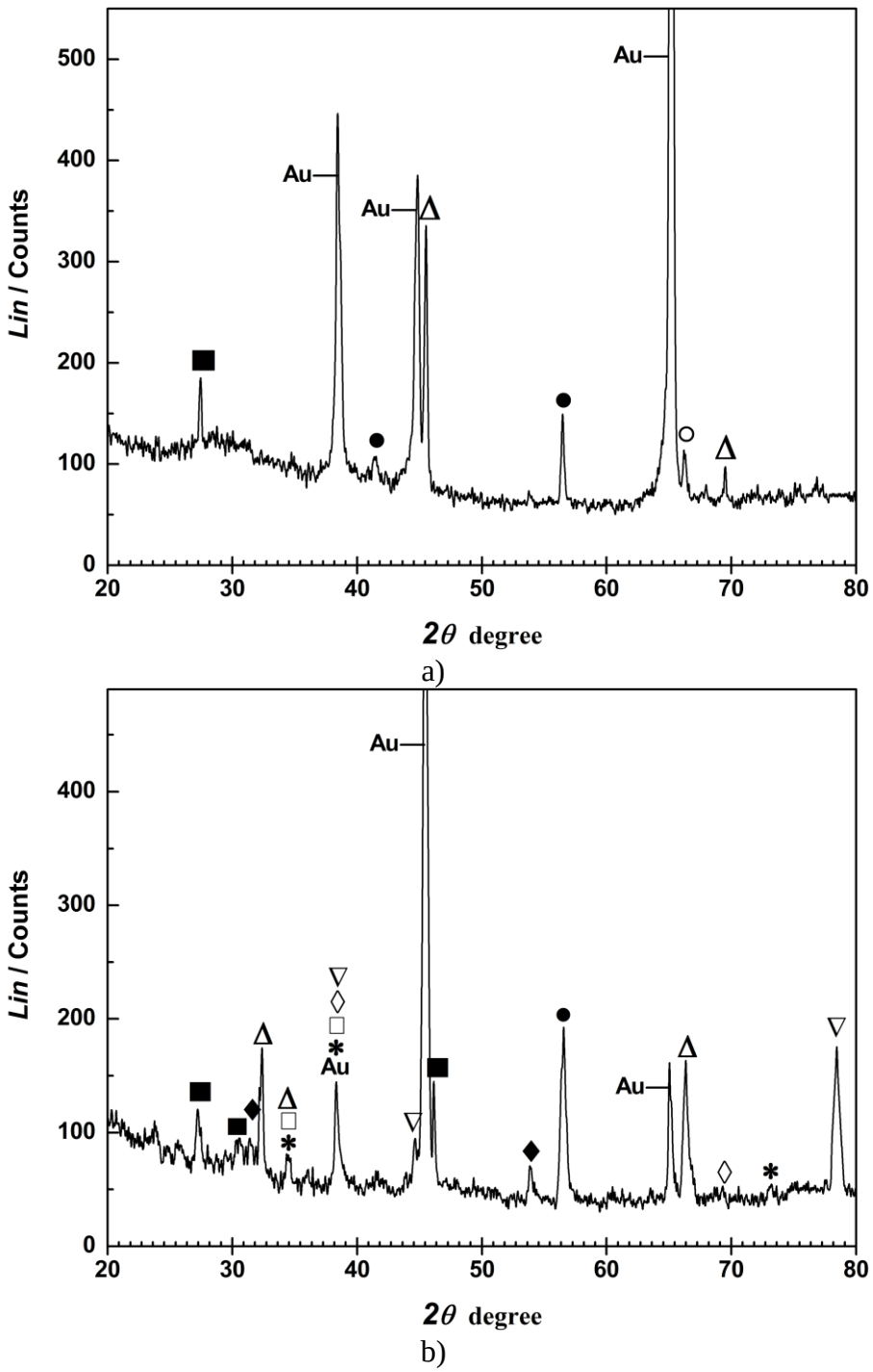

Figure 10. a) XRD spectra of the Au electrode held for 2 h under the potential of E = − 0.050V vs. Al in equimolar melt $AlCl_3$+NaCl containing anodically dissolved Nb; T = 473 K: **(Au)**-Au [39]; (■)-AlAu [44]; **(●)**-$AlAu_4$ [45]; **(o)**-$AlAu_2$ [42]; **(Δ)**-$AlNb_2$ [43]; b) XRD analysis of the Au surface after 1h under potential of E = − 0.100V vs. Al in the same melt as above; T = 473 K: **(Au)**-Au [39]; (■)-AlAu [44]; **(Δ)**-$AlNb_2$ [43]; **(□)**-$AuNb_3$ [49]; **(*)**-$AlNb_3$ [41]; **(◊)**-Nb [46]; (▽)-Al [50]; **(♦)**-Au_2Nb_3 [40]; (●)-$AlAu_4$ [45].

EDS analysis of the surface of the gold electrode obtained under conditions described in Fig. 10. a) is given in Fig.11. a) and b). The SEM photo, Fig.11 a) shows coarse metallic deposits consisting mainly of aluminium and niobium, Fig. 11b). Aluminium is dominant, although niobium is

deposited under higher cathodic overpotential (about −200 mV vs. Nb), because Nb deposits with limited current.

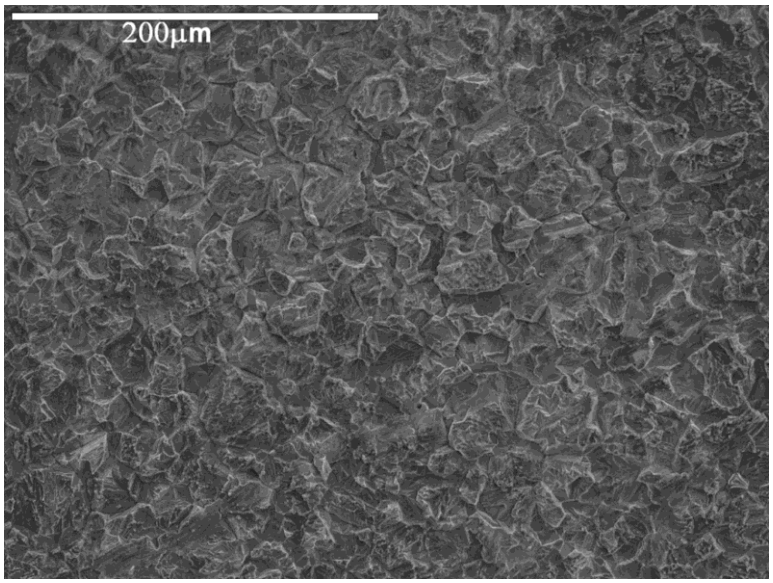

a)

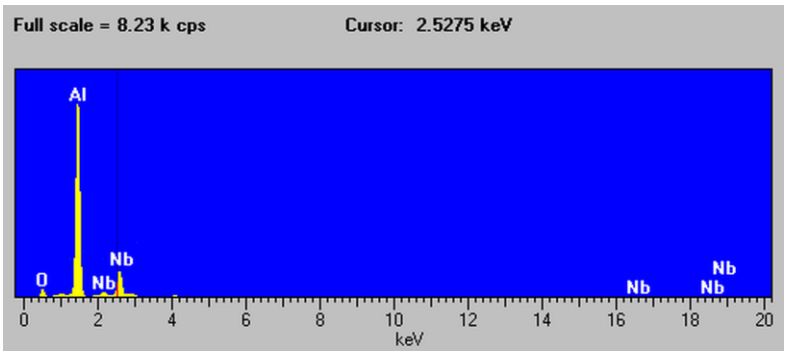

b)

Figure 11. a) SEM photo of the Au surface after being held for 2 h at potential E = − 0.050 V vs. Al in the melt of equimolar mixture $AlCl_3$+NaCl with anodically dissolved Nb, T = 473 K (magnification 300x); b) EDS analysis of the sample given as a).

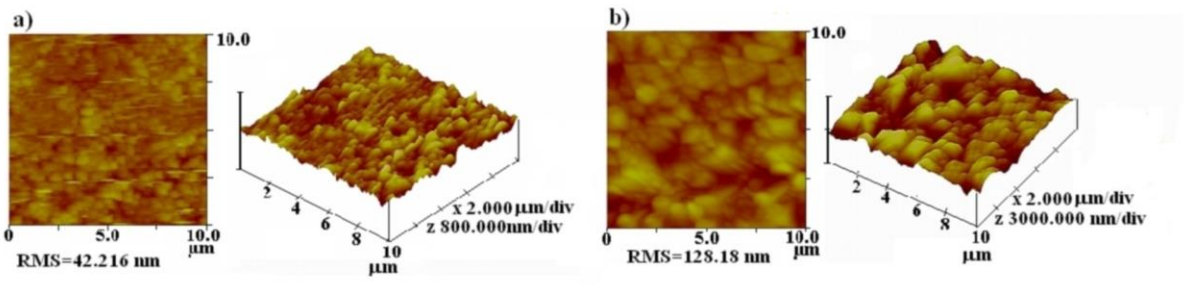

Figure 12. 2D (bird's view) and 3D (profile) of the Au electrode surface (AFM analysis); a) before (10 µm x 10 µm x 1.5 µm); b) after 2 hours of E = −0.050 V vs. Al applied in eqiumolar melt $AlCl_3$+NaCl with anodically dissolved Nb,T = 473 K, (10 µm x 10 µm x 1.5µm).

AFM of the surface obtained under the same conditions is presented in Fig. 12. Increase in RMS (coarseness of the surface) is obvious and should be attributed to aluminium and niobium deposits.

SEM appearance of the aluminium and niobium deposits obtained under constant potential of – 100 mV vs. Al for one hour from the melt at 473 K are presented in Fig. 13.a) and EDS analysis of the samples is shown in Fig. 13.b).

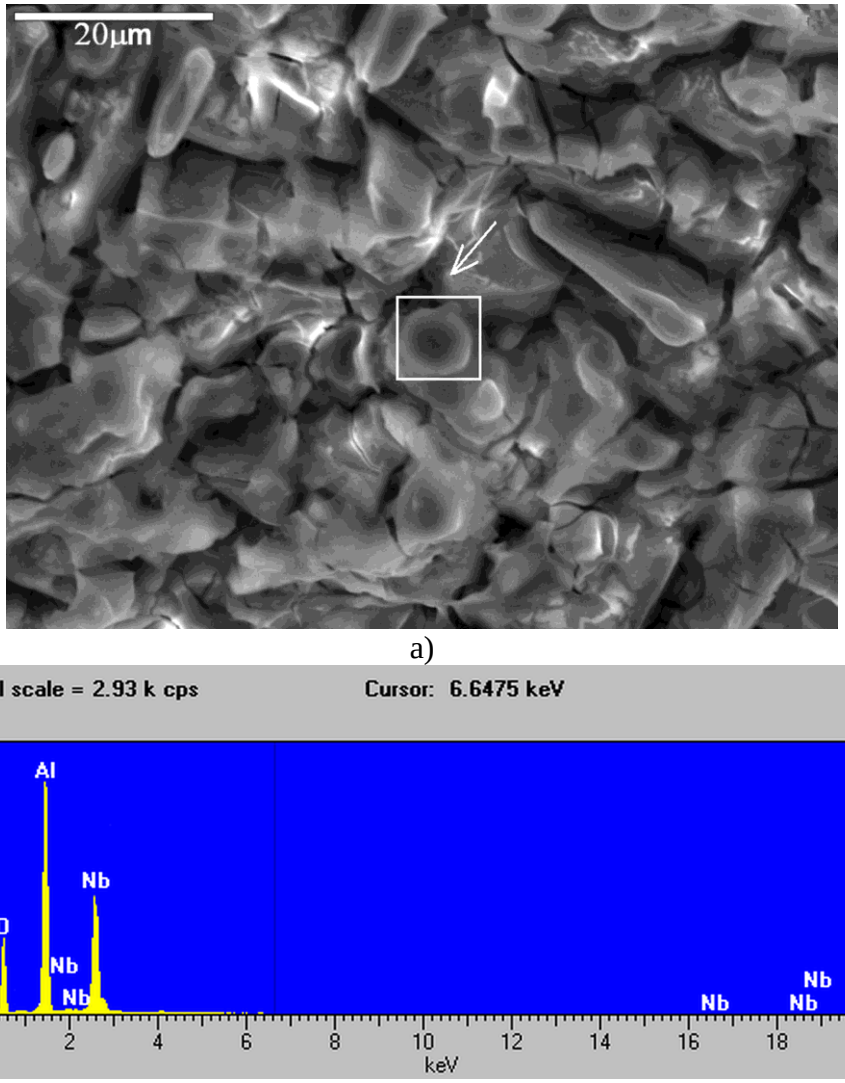

a)

b)

Figure 13. SEM of the Au surface after one hour of E = – 0.100 V vs. Al potential applied in equimolar $AlCl_3$+NaCl melt enriched with anodically dissolved Nb; T = 473 K; a) magnification 1500; b) EDS analysis of the sample given as a).

EDS results evidently recognize aluminium and niobium as participants in the deposits. Surface morphologies of the gold sample, before and after niobium-aluminium deposition at 473 K of one hour, analysed by AFM, are presented in Fig. 14.a) and b). The surface after niobium-aluminium codeposition on gold shows agglomerations of different sizes and a significant increase in roughness.

In the relevant literature there is evidence of attempts to electrodeposit niobium on graphite, vitreous carbon, diamond, steel, Ni, Mo, Mg, W, Nb, Pt, Fe, Cu, etc., from melts made of different combinations of Na, K, Li, Cs, Ca, Al chlorides and fluorides.

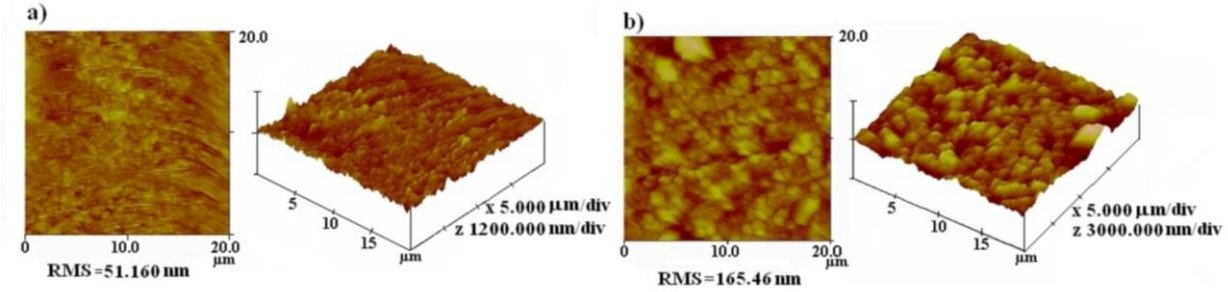

Figure 14. 2D and 3D AFM images of the gold surface: a) before niobium-aluminium deposition; b) after one hour niobium-aluminium deposition at 473 K, at – 0.100V vs. Al.

Some of those works report Nb-Sn [51], Nb-Ti [52], Nb-Hf [8], Nb-Al [17,23,34,53] and Nb-C [8,54] alloys being formed between Nb deposited (from chloride, fluoride melts and ionic liquids) and substrate used as a cathode. However, there are only a few reports [16,17,23,30,34,53,55,56] describing Al and Nb co-deposition resulting in Nb-Al alloy formation and those are from chloride and fluoride melts on W, Cu and Nb cathode, but not on Au. LSV and SEM results reported in some of the works [30,55,56] are similar to ours. Of course, actual values of the potentials recorded differ with chemical compositions of the melt and substrate used. The morphology of the deposits was very similar to ours but authors did not discuss chemical and crystallographic composition of the deposits obtained. Voltammograms, potentials recorded and SEM photos in works done on tungsten in Na–Al chloride melts [16,17,34] are similar to ours, but no underpotential deposition was reported or alloys identified. Work done with a W cathode in Li-K-Al-Nb chloride melts [23] shows similar LSV results; Al-Nb alloy formation and Al underpotential deposition on an Nb substrate. Some of the above mentioned substrates (Pt, Ni, Ag, Cu) including Au were also used as working electrodes in Nb chlorides-ionic liquids electrolytes for deposition of niobium [24-31,55].

An attempt to obtain superconductive Nb_3Al alloy by electrodeposition of Nb and Al from NaCl-52mol% $AlCl_3$ onto tungsten ended in alloys with Nb:Al wt% ratio equal to approximately 1:2 [16]. Another report [23] describes formation of thick, Nb reach, compact $Nb_{1-x}Al_x$ alloy on the Pt substrate by electrochemical codeposition of Nb and Al from LiCl-KCl eutectic melt. There is a report [34] on Nb-Al alloy formation containing 3-13.4% of Nb obtained by electrodeposition of Nb and Al onto tungsten from 52mol% $AlCl_3$+ 48mol% NaCl melt.

The deposits obtained in our work are listed in Table 2, as a function of applied potentials. Gold-aluminium, gold-niobium and aluminium-niobium alloys recorded at potentials more anodic than 0.150 V vs. Al suggest underpotential deposition of both aluminium and niobium on gold. Underpotential deposition of aluminium onto gold substrates has been reported earlier [36] but niobium underpotential deposition on gold was not. However, according to Kolb at al. hypothesis

[37,38] the niobium underpotential deposition on gold is as probable as aluminium underpotential deposition on gold.

It is diffusion of the material of underpotentially deposited atomically thin layers of Al and Nb, between themselves and gold substrate that is responsible for the formation of recorded alloys. The chemical bond between the transition metal (Nb) and the s-p metal (Al) is known to be rather strong and according to the Nb-Al phase diagram, there is finite solid solubility of Al in Nb (about 8 at.% AI) [57] hence, according to XPS results, presence of atomic diffusion cannot be ruled out. Maximum solubility of Al in Nb is reported to be between 15 at.% to 23 at.% and decreases appreciably with decrease of temperature [58] and solid solubility of niobium in aluminium is limited to 20% wt. Nb at peritectic temperature decreasing to less than 0,1% at 600 K [59]. The homogeneity range for $AlNb_3$ is also very restricted, while $AlNb_2$ homogeneity range spans from ≈ 65 to 75 at.% Nb. $AlNb_2$ is the only observed phase to have a range of homogeneity [58]. Recently some authors proposed a revised equilibrium Nb-Al phase diagram because of an Nb_3Al and Nb_2Al euthectoidal transformation reaction into bcc Al-Nb solid solution. According to them, at lower temperatures, all published equilibrium phase diagrams show stoichiometric compositions for equilibrium [60]. By the way, best superconductor properties of Nb_3Al structure can be obtained only by stoichiometric composition of Nb-Al equilibrium phase when the A15 phase has the composition close to 25 at.% Al [61].

Table 2. Deposits formed at different potentiostatic regime on Au electrode from equimolar melt $AlCl_3$+NaCl with anodically dissolved Nb.

Applied potential	Au – Nb alloys	Au – Al alloys	Al – Nb alloys
0.150 V vs. Al	Au_2Nb_3	$AlAu_2$	$AlNb_2$
			$AlNb_3$
0.100 V vs. Al	Au_2Nb	$AlAu_4$	$AlNb_2$
	Au_2Nb_3	AlAu	
- 0.100 V vs. Al	$AuNb_3$	$AlAu_4$	$AlNb_2$
	Au_2Nb_3	AlAu	$AlNb_3$
		$AlAu_2$	

Alloys formed at potentials equal or more negative than the niobium reversible potential in the system used included those formed as a consequence of Al and Nb underpotential deposition and those by niobium overpotential deposition (Table 2.) all of which were formed by interdiffusion. The Au-Nb intermetallics formed by overpotential Nb deposition obtained by other authors, were results of direct and selective diffusion of Nb into Au and vice versa [61] or heavy mechanical impact in high energy ball mill [62]. These methods should not come as a surprise as the maximum solubility of Nb in Au is about 57at% and the maximum solubility of Au in Nb is about 36 at%. All three recorded phases, Au_2Nb, Au_2Nb_3, $AuNb_3$, are stable bellow 1223 K [63].

At potentials more negative than the reversible potential of aluminium and niobium, the Al-Nb co-deposition region, deposition of niobium proceeds under limited current and that might be the

reason for relatively small proportion of Al-Nb alloys formed. Thicker $AlNb_2$, $AlNb_3$ layers have been achieved by other different methods as well [64,65].

4. CONCLUSIONS

Niobium and aluminium have been electrodeposited on gold substrate at 473 K from melts made of equimolar mixture $AlCl_3$+NaCl with niobium added by anodic dissolution. Underpotential deposition of both, aluminium and niobium was recorded at potentials more positive than reversible potentials of niobium. It was found that these underpotential depositions on gold precede overpotential deposition of niobium and subsequently aluminium.

Niobium was overpotentially deposited individually and co-deposited with aluminium.

Electrochemical techniques applied (LSV, polarization, open circuit and potential step) indicated and physical analytical methods (SEM, EDS, AMF and XRD) confirmed formation of several niobium-aluminium ($AlNb_2$, $AlNb_3$), niobium-gold (Au_2Nb, Au_2Nb_3, $AuNb_3$) and aluminium-gold alloys (AlAu, $AlAu_2$, $AlAu_4$) in niobium and aluminium underpotential, niobium overpotential as well as in niobium and aluminium overpotential co-deposition regions.

Alloys obtained were formed at temperatures several hundred degrees Celsius lower than the temperatures which are, according to the relevant existing binary phase diagrams, needed for their formation by thermal means.

References

1. G. W. Mellors and S. Senderoff, *J. Electrochem. Soc*., 112 (1965) 266.
2. A. Girginov, T. Z. Tzvetkoff and M. Bojinov, *J. Appl. Electrochem*., 25 (1995) 993.
3. B. Kubikova, V. Danek and M. Gauene-Escard, *Z. Naturforsch.*, 62a (2007) 540.
4. M. Chemla and V. Grinevitch, *Bull. Soc. Chim. Fr*., 3 (1973) 853.
5. N. Jovićević, V. S. Cvetković, Ž. Kamberović and T. S. Barudžija, *Int. J. Electrochem. Sci.,* 10 (2015) 8959.
6. V. Danek, M. Chrenkova, D. K. Nguyen, V. Viet, A. Sylny, E. Polyakov and V. Kremenetsky, *J. Mol. Liq*., 88 (2000) 277.
7. S. A. Kuznetsov, *Pure Appl. Chem*., 81 (2009) 1423.
8. D. Chen, F. Deng, C. Ding, Y. Wang and H. Li, *Int. J. Electrochem. Sci.,* 10 (2015) 9015.
9. I. Nowak and M. Ziolek, *Chem. Rev*., 99 (1999) 3603.
10. N. Koizumi, T. Takeuchi and K. Okuno, *Nucl. Fusion,* 45 (2005) 431.
11. J. Wadsworth and F. H. Froes, *JOM*, 41 (1989) 12.
12. S. Senderoff and G. W. Mellors, *J. Electrochem. Soc.,* 113 (1966) 66.
13. G. Ting, K. W. Fung and G. Mamantov, *J. Electrochem. Soc*., 123 (1976) 624.
14. F. Lantelme and Y. Berghoute, *J. Electrochem. Soc*., 141 (1994) 3306.
15. K. D. Sienerth, E. M. Hondrogiannis and G. Mamantov, *J. Electrochem. Soc.,* 141 (1994) 1762.
16. Y. Sato, K. Iwabuchi, N. Kawaguchi, H. Zhu, M. Endo, T. Yamamura and S. Saito, *Cathodic behavior of the deposition of Nb and Al in NaCl-$AlCl_3$ melt, Tenth International Symposium on Molten Salts*, Los Angeles, USA, 1996, pp. 179-188.
17. V. Van, A. Silny, J. Hiveš and V. Danek, *Electrochem. Comm.,* 1 (1999) 295.
18. V. Van, A. Silny and V. Danek, *Electrochem. Comm*., 1 (1999) 354.

19. L. P. Polyakova, T. V. Stogova, E. G. Polyakov, A. V. Arakcheeva and V. V. Grinevich, *Plasmas & Ions,* 3 (2000) 21.
20. C. Rosenkilde, A. Vik, T. Ostvold, E. Christensen and N. J. Bjerrum, *J. Electrochem. Soc*., 147 (2000) 3790.
21. V. V. Grinevich, A. V. Arakcheeva and S. A. Kuznetsov, *J. Min. Metall. Sect. B,* 39 (2003) 223.
22. A. V. Popova, S. A. Kuznetsov and V. Standard, *Russ. J. Electrochem.,* 48 (2012) 93.
23. M. Mohamedi, N. Kawaguchi, Y. Sato and T. Yamamura, *J. Alloys Compd.,* 287 (1999) 91.
24. I. W. Sun and C. L. Hussey, *Inorg. Chem.,* 28 (1989) 2731.
25. R. Quigley, P. A. Barnard, C. L. Hussey and K. R. Seddon, *Inorg. Chem.,* 31 (1992) 1255.
26. W. E. O'Grady, D. F. Roeper, K. I. Pandy and G. T. Cheek, *Powder Diffr.,* 26 (2011) 171.
27. G. T. Cheek, H. C. De Long and P. C. Trulove, *Electrodeposition of Niobium and Tantalum from a Room-Temperature Molten Salt System*, *Proceedings of the International Symposium on Molten Salts XII*, Honolulu, USA, 1999, pp. 527-534.
28. O. B. Babushkina, E. O. Lomako and W. Freyland, *Electrochim. Acta,* 62 (2012) 234.
29. A. I. Wixtrom, J. E. Buhler, C. E. Reece and T. M. Abdel-Fattah, *ECS Trans.,* 50 (2012) 225.
30. P. Giridhar, S. Zein El Abedin, A. Bund, A. Ispas and F. Endres, *Electrochim. Acta,* 129 (2014) 312.
31. A. Vacca, M. Mascia, L. Mais, S. Rizzardini, F. Delogu and S. Palmas, *Electrocatalysis,* 5 (2014) 16.
32. J. N. von Barner, N. J. Bjerrum and G. P. Smith, *Acta Chem. Scand. Ser. A,* 32 (1978) 837.
33. R. Huglen, G. Mamantov, G. P. Smith and G. M. Begun, *J. Raman Spectrosc.,* 8 (1979) 326.
34. G. R. Stafford and G. M. Haarberg, *Plasmas& Ions,* 2 (1999) 35.
35. R. S. Nicholson and I. Shain, *J. Anal. Chem.,* 36 (1964) 706.
36. B. S. Radović, R. A. H. Edwards and J. N. Jovićević, *J. Electroanal. Chem.,* 428 (1997) 113.
37. H. Gerischer, D. M. Kolb and M. Przasnyski, *Surf. Sci.,* 43 (1974) 662.
38. D. M. Kolb, M. Przasnyski and H. Gerischer, *J. Electroanal. Chem.,* 54 (1974) 25.
39. ICDD PDF-2, 03-065-2870, The International Centre for Diffraction data, 2003.
40. ICDD PDF-2, 00-029-0650, The International Centre for Diffraction data, 2003.
41. ICDD PDF-2, 00-029-0650, The International Centre for Diffraction data, 2003.
42. ICDD PDF-2, 00-026-1006, The International Centre for Diffraction data, 2003.
43. ICDD PDF-2, 00-012-0615, The International Centre for Diffraction data, 2003.
44. ICDD PDF-2, 00-030-0019, The International Centre for Diffraction data, 2003.
45. ICDD PDF-2, 03-065-4893, 00-006-0576, The International Centre for Diffraction data, 2003.
46. ICDD PDF-2, 01-089-3715, The International Centre for Diffraction data, 2003.
47. ICDD PDF-2, 03-065-7803, The International Centre for Diffraction data, 2003.
48. ICDD PDF-2, 01-082-1142, The International Centre for Diffraction data, 2003.
49. ICDD PDF-2, 03-065-4239, The International Centre for Diffraction data, 2003.
50. ICDD PDF-2, 01-089-2769, The International Centre for Diffraction data, 2003.
51. S. Franz, E. Barzi, D. Turrioni, L. Glionna and M. Bestetti, *Mater. Lett.,* 161 (2015) 613.
52. L. P. Polyakova, P. Taxil and E. G. Polyakov, *J. Alloys Compd*., 359 (2003) 244.
53. O. Rebrin, I. V. Polovov, V. A. Volkovich, A. S. Muhamadeev and A. V. Chernoskutov: *Electrochemical Behaviour of Niobium and Aluminium in Chloride Melts*, *206th ECS Meeting,* Honolulu, USA, 2004, pp. 1037-1045.
54. F. Lantelme, A. Salmi, B. Coffin, J. Claverie and Y. Le Petitcorps, *Mater. Sci. Eng. B,* 39 (1996) 202.
55. M. Mascia, A. Vacca, L. Mais, S. Palmas, E. Musu and F. Delogu, *Thin Solid Films,* 571 (2014) 325.
56. K. Koura, T. Kato and E. Yumoto, *J. Surface Finish. Soc. Jpn.,* 4 (1994) 805.
57. M. Gurvitch and J. Kwo, *Advanced in Cryogenic Engineering Materials*, Springer US, (1984) New York, USA.

58. R. P. Elliiott and F. A. Shunk, *Bull. Alloy Phase Diag.*, 2 (1981) 75.
59. L. F. Mondolfo, *Aluminium Alloys: Structure and Properties*, Butterworths, (1976) London-Boston, USA.
60. F. Buta, M. D. Sumption and E. W. Collings, *IEEE T. Appl. Supercon.*, 13 (2003) 3462.
61. P. Müller, *Phys. Stat. Sol. (a)*, 49 (1978) K75.
62. L. M. Di and H. Bakker, *Appl. Phys. Lett.*, 62 (1993) 429.
63. H. Okamoto and T. B. Massalski, *Bull. Alloy Phase. Diag.*, 6 (1985) 134.
64. K. Matsuura, T. Koyanagi, T. Ohmi and M. Kudoh, *Mater. Trans.*, 44 (2003) 861.
65. X. Y. Yan and D. J. Fray, *J. Alloys Compd.*, 486 (2009) 154.